Received: 13 February 2023 | Accepted: 28 September 2023

DOI: 10.1111/arcm.12922

ORIGINAL ARTICLE

The modeling pastes of the monumental *terracruda* sculpture of the Silk Roads: Archaeometric study of the Tepe Narenj and Qol-e-tut examples (Kabul, Afghanistan)

Monica López-Prat[1,2] | **Raffaella De Luca**[3] | **Alessandra Pecci**[2,4,5] | **Simona Mileto**[4] | **Sudipa Ray Bandyopadhyay**[6] | **Andrea Bloise**[3] | **Adriano Guido**[3] | **Mara Cipriani**[3] | **Carla Lancelotti**[7,8] | **Begoña Carrascosa**[9] | **Noor Agha Noori**[10] | **José-Manuel Simón-Cortés**[9] | **Domenico Miriello**[3,11]

[1]Department of Arts and Conservation, Conservació - Restauració del Patrimoni Research Group, Universitat de Barcelona, Barcelona, Spain

[2]Institut d'Arqueologia de la Universitat de Barcelona, Barcelona, Spain

[3]Department of Biology, Ecology and Earth Science, University of Calabria, Rende, Italy

[4]ERAAUB, Departament d'Història i Arqueologia, Universitat de Barcelona, Barcelona, Spain

[5]INSA-UB, Institut de Recerca en Nutrició i Seguretat Alimentària de la Universitat de Barcelona, Barcelona, Spain

[6]Department of Ancient Indian History and Culture, University of Calcutta, Calcutta, India

[7]CaSEs Research Group, Department of Humanities, Universitat Pompeu Fabra, Barcelona, Spain

[8]ICREA, Catalan Institution for Research and Advanced Studies, Barcelona, Spain

[9]Institut Universitari de Restauració del Patrimoni, Universitat Politècnica de València, València, Spain

[10]Archaeology Institute of Afghanistan, Kabul, Afghanistan

[11]Collaborator of the Institut d'Arqueologia de la Universitat de Barcelona (IAUB), Barcelona, Spain

Correspondence
Monica López-Prat, Department of Arts and Conservation, Conservació - Restauració del Patrimoni Research Group, Universitat de Barcelona, Barcelona, Spain.
Email: monica.lopez@ub.edu

Funding information
This research has been supported by a National Geographic Society Early Career Grant (EC-59568C-19). MCIN (Ministerio de Ciencia e Innovación)/AE (Agencia Estatal de Investigación); 10.13039/501100011033) and

Abstract
This paper presents the results of the mineralogical, petrographic and chemical study of different archaeological samples related to terracruda sculptures and other elements that were part of the architectural decoration of the Buddhist sites of Tepe Narenj and Qol-e-tut (Kabul, Afghanistan; fifth to 11th centuries CE). The main objective of the study was to characterize the samples using an archaeometric approach. The study helped to

"Next Generation EU"/PRTR. Grant number: FCJ2021-046803-I.

[Correction added on 13 November 2023, after first online publication: MCIN/AE and "Next Generation EU"/PRTR funding information has been added.]

better understand the materials involved in the modeling of Afghan sculptures and their processing, such as the different nature of the clay layers and the finishing 'stucco' coating. The results further indicate that similarities exist among the manufacturing process of the studied samples and that used today by an ancient caste of clay artists in West Bengal (India), suggesting the existence of a continuous technological tradition that deserves to be further explored in the future.

KEYWORDS

Afghanistan, archaeometry, clay, heritage conservation, organic binders, silk roads, stucco, terracruda sculpture, traditional knowledge

INTRODUCTION

This paper presents the results of the archaeometric study of samples from different clay-based architectural elements (sculptures, mural paintings, reliefs, and walls) from the Buddhist archaeological sites of Tepe Narenj and Qol-e-tut (Kabul, Afghanistan; fifth to 11th centuries CE). The study involved mineralogical, petrographic, and chemical analysis of the samples, and is part of a broader interdisciplinary research project that aims to better understand terracruda sculptures from a technological point of view (López-Prat et al. 2021; López-Prat, Agostina, et al. 2022; López-Prat, Lancelotti, et al. 2022).

The sculptural fragments studied can be considered archaeological examples of an artistic tradition of modeling monumental terracruda (made with air-dried or unfired clay, in contrast to fired clay or terracotta) sculptures that, to our knowledge, has never been practiced outside South, Central, and Eastern Asia, and it is geographically connected to the so-called Silk Roads. Although no scientific proof exists on the presence of a unique technological tradition, in order to better understand the manufacture of these sculptures, we took into account what is currently known both from written sources and from Indian traditional sculpture modeling. In fact, although very distant in time and geographic area, some studies suggest that at least part of the production process may have been similar. In particular, the Indian scholar K. M. Varma (1970) in his work, *The Indian technique of clay modelling*, stated that the ancient tradition of making unfired-clay sculptures with world-famous examples attributed to the 'Art of Gandhara' (developed in the northwest of the Indian subcontinent—modern day Pakistan and Afghanistan—in the first centuries of the common era), was still alive in West Bengal (India). There, according to Varma, an ancient caste of clay artists continues to produce terracruda sculptures following a century-old tradition described in the Agamas, a collection of Sanskrit texts mentioning the preference of unfired clay to create the image of divinity, the oldest dating back to the eighth century CE (Varma, 1970). On the other hand, punctual ethnographic observations carried out by López Prat in West Bengal (India) allowed the documentation of the different phases of the production of modern Bengali terracruda sculptures, which seem to corroborate such similarities (López-Prat et al., 2021).

Considering all this information, the study presented in this paper was aimed at providing relevant data to elucidate some of the open questions about the technology and materials used in the production of the ancient Afghan sculptures. We wanted to understand if there were different layers of clay-based pastes in the same sculpture, and their nature (coarser/smoother; Blänsdorf & Melzl, 2009; Klimburg-Salter, 2018; Tarzi, 1986; Verardi, 1983), the composition of the material commonly known as 'stucco' (which is supposed to be lime or gypsum-based;

Middleton & Gill, 1996; Tarzi, 1986; Varma, 1987; Verri et al., 2019) and the addition of binding organic substances in the stucco or the clay-based pastes (Bonaduce et al., 2009; Forgione, 2019; Lluveras-Tenorio et al., 2022; Pannuzi et al., 2019). All of these data are of great relevance in addressing the design of conservation interventions on historic-archaeological examples. We addressed these questions through different diagnostic techniques, including optical microscopy (OM), X-ray powder diffraction (XRPD), differential scanning calorimetry and thermogravimetry (DSC/TG), Eenergy dispersion microanalysis by scanning electron microscope (SEM-EDS), electron probe micro-analysis (EPMA/EDS), raman spectroscopy, epifluorescence analysis and preliminary gas chromatography/Mass spectrometry (GC/MS).

The tradition of modeling monumental terracruda sculptures: from antiquity to nowadays

As mentioned in the introduction, the sculptural fragments under study can be considered archaeological artifacts belonging to the artistic tradition of modeling monumental terracruda sculptures practiced in South, Central, and Eastern Asia. Examples of this artistic expression are mainly linked to the spread of Buddhist art from the northwest of the Indian subcontinent through what is known today as the 'Silk Roads'. The first Buddhist instances are found at the beginning of the common era in the area of present-day southern Uzbekistan, Tajikistan, Afghanistan, and Pakistan, linked to the world-renowned "Art of Gandhara." Later, they spread to the Himalayas and Eastern Asia, where examples can be identified up to modern times.

If we try to synthesize the available information on the characteristics that might be identified with a common manufacturing pattern, these sculptures would be made by the following essential components:

- a core structure made of brick, stone, wood, or reeds anchored to the wall or pavement (and forming part of it in the case of brick or stone);
- several layers of overlapping 'clay' ranging from thickest to finest, on which the details of the decoration were molded or stamped;
- a finishing coat usually identified as 'stucco' if white;
- gold and/or polychrome decoration.

These essentials elements allowed the creation of sculptures skillfully modelled in situ as part of monuments or architectures that could be smaller than human size or reach several meters in height, finished with great quality and in high detail but extremely heavy and fragile.

In turn, the *Agamic* literature (a collection of Sanskrit scriptures ranging from the eighth to the 17th centuries CE and belonging to several Hindu devotional schools) deals with the artistic ritual of modeling the divinity in (unfired) clay. According to Varma, these texts mention the preparation of the modeling pastes and the surface finishes: "the clay (mrt) is selected from rivers, ponds and lakes and must be well cleaned. It is obtained from three types of soil: *jangala* (sandy soil); *anupa* (moist soil); *misra* (mixed soil, neither hard nor soft and contains a small amount of sand and relative stickiness)" (Varma, 1970, p. 19). The various types of clay must be obtained from these three types of soil and must be prepared separately, following 12 steps that result in a long process during which, in short, the clay is first filtered and decanted, and then numerous products of various origins are added at different stages. In the last stage, the 12th, coconut husk fibers must be cut and added to the clay in a ratio of 1:4. All these products must be processed and mixed according to specific instructions, exact proportions, long kneading, and resting times, so that the preparation of the various clays alone would comprise several weeks of work. According the texts, the inner layers are assembled with the wettest type of clay (*anupa*). Once this is dry, the second type of mixed clay (*misra*) combined with the addition of ropes is added and when this is well dry, the third type of clay (*jangala*) is overlapped (Varma, 1970, p. 87). These texts also mention the preparation of the finishing surface prior to polychromies, which is obtained by grinding *sarkaras* (translated by Varma as gravel or pebbles) agglutinated with organic binders mixed with cotton fibers in various proportions to obtain three types of consistency for the paste (*kalka*), producing a preparation named *sarkara-kalka* (the *sarkara* paste) (Varma, 1970, pp. 88–89). According to agamic literature, the *sarkara-kalka* must be applied in layers of decreasing density with intermediate drying processes and include, in the middle of the process, the addition of cotton fabric dipped in the secretion of the *Limonia acidissima L.* (wood apple or kawista, *Feronia elephantum* as translated by Varma from the original text). Once the layer of fabric is overlapped, three more layers of *sarkara-kalka*, much more liquid than the previous ones and without cotton fibers, are applied (Varma, 1970, p. 89).

Ethnographic observations carried out in west Bengal (India) allowed to understand the current processing method of monumental terracruda sculptures performed by an ancient caste of clay sculptors (the *kumors*) (López-Prat et al., 2021), suggesting that it may share some similarities with the artistic ritual described in Varma's work. Bengali sculptors use three types of clay (*mati*) either mixed with different herbaceous materials and resins or not depending on the different layers necessary to achieve the whole body of the sculpture. In Kumortuli (Kolkata, West Bengal), these different kinds of clay are:

- *bele-mati* or *gonga-mati* (a sandy clay extracted from the Hoogly River, a distributary of the Ganges River and the western Kumortuli border),
- *etel-mati* (stickier and brought by boat from the Diamond Harbour area in the southern suburb of Kolkata where the Hoogly meets the Bay of Bengal),
- and *kore-mati* or 'Chinese clay' (a type of commercialized chalk or kaolinite).

Etel-mati is mainly used to model the internal layers of the idols, and it is first sieved and filtered in a purifying process before being mixed with rice husk and rice straw (this last mostly in the case of large or colossal sculptures). *Bele-mati* is used to model the external layers of the sculpture.

Sculptors sometimes mix *etel-mati* and *bele-mati* to achieve specific properties of the modeling pastes, mainly in the making of faces, hands or decorations involving the use of plaster molds. The total number of layers of a sculpture varies according to the total size of the body. Finally, *kore-mati* is prepared by diluting grinded chalk or kaolinite in water and mixing it with a gum made from boiling tamarind seeds and other 'secret' products that vary from one workshop to another and that allow to obtain the final shining of the polychrome by rubbing this external layer with a cotton cloth only. The main goal of applying the different layers based on *kore-mati* (the most external mixed with the color associated to the divinity represented) is to prepare the sculpture for painting (López-Prat et al., 2021).

The monumental terracruda sculptures of Tepe Narenj and Qol-e-tut

Tepe Narenj and Qol-e-tut are two Buddhist sites, separated by ca. 400 m. laying on the eastern slopes of the Hindukush Mountain chain, only a few kilometers to the south of the present-day city of Kabul, overlooking the natural lake of Qol-e-Hashmat Khan. According to previous archaeological research, directed by the archaeologist Z. Paiman and coordinated by the Archaeological Institute of Afghanistan, Tepe Narenj was the location of a Buddhist monastery that was active between the fifth and 10th centuries CE. The excavations carried out between 2004 and 2011 uncovered an architectural complex system of terraces with three levels (lower, middle, and upper) interconnected by a system of steps and platforms (Paiman, 2012). On the terraces in the middle portion of the site stood a series of cult chapels with the remains of multiple examples of monumental terracruda sculptures preserved. The ensembles documented at Tepe Narenj consist of life-size or colossal figures placed inside chapels and linked to iconographic programs of Buddhist cosmology, some of them identified with the Tantric tradition (Paiman, 2010).

According to archaeological research, Qol-e-Tut was also a monastic complex active between the sixth and the 11th centuries CE (Paiman, 2018). Excavations carried out between 2008 and 2013 revealed a complex network of buildings arranged on terraces, where several chapels, two stupas, and various monastic cells were erected. The architectural remains presented mural paintings and important sculptural findings. To date, the presence of sculptures at Qol-e-tut is essentially represented by large feet preserved in situ on pedestals, highlighting a colossal polychromed Buddha in its original position erected in Chapel 13, two small figures in Chapel 15, and many sculptural fragments recovered during the excavation and preserved in the various rooms of the monastic complex.

Tepe-Narenj and Qol-e-tut are two of the best surviving examples of Afghan Buddhist archaeology, especially because of the importance of the preserved in situ monumental sculptural decoration linked to Gandharan art. These sculptures were modelled following the aforementioned essentials, which in these cases and roughly speaking, involved the use of a core skeleton of wood, followed by different layers of clay-based pastes, sometimes preserving a thin final coat of gypsum-based stucco that exceptionally retained traces of color (Figure 1).

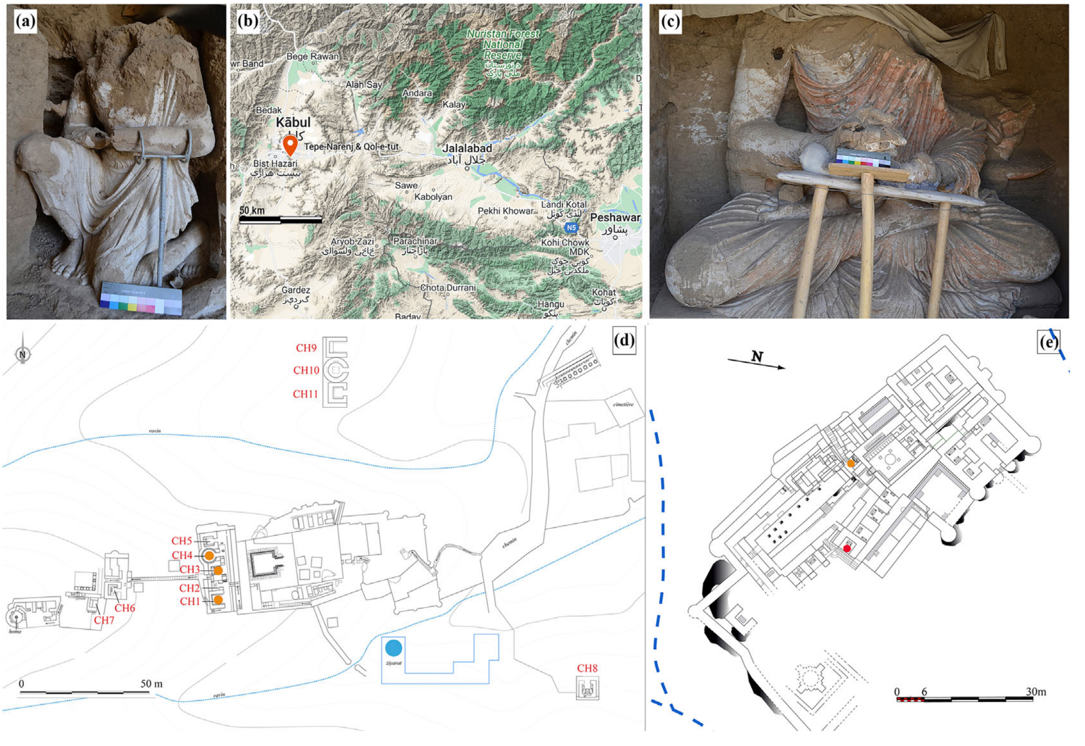

FIGURE 1 (a) Example of monumental terracruda sculpture from Chapel 3 of Tepe Narenj. (b) Location of Tepe Narenj and Qol-e-tut. (c) Colossal polychromed Buddha of Qol-e-tut. (d) Map of Tepe Narenj highlighting the chapels and the original location (highlighted with orange dots) of the studied samples TN1toTN6. (e) Map of Qol-e-tut highlighting the original location of the studied samples. The orange dot corresponds to the original location of the samples QT1, QT2, and QT3 (Chapel 13), and the red dot to the QT4 (Chapel 6). Maps courtesy of Z. Paiman.

The monumental terracruda sculptures, once the buildings or monuments where they were inserted are abandoned, undergo a process of degradation and, during the archaeological interventions, it is common that:

- the sculptures appear fragmented in the sediment associated with the rubble,
- the remains are preserved within the area where they were found awaiting restoration of the surrounding sculptures.

This is the case of Tepe Narenj and Qol-e-tut, where, once recovered, many of the sculptural remains were preserved in the different rooms where they were found, awaiting a hypothetical restoration that was supposed to replace them in their original position as part of the surrounding sculptures still preserved in situ.

MATERIALS AND METHODS

Sampling

Samples were recovered from fragmented sculptures at the two monasteries in the sediment associated with the rubble within the area where the sculptures were found.

Sampling was carried out in July 2018, thanks to an agreement between the Archaeological Institute of Afghanistan (AIA) and the Polytechnique University of Valencia (UPV). Sampling was based on the premise of not damaging the remains still in situ and according to a criterion of morphological and functional representativeness based on the findings preserved in the different chapels of the two monastic complexes studied. In addition to terracruda sculpture pieces, fragments from mural surfaces (with and without decoration) were also collected to observe potential technical differences between the different architectural elements. The sculptural fragments were selected with the aim of studying a spectrum of the diverse typologies preserved in Tepe Narenj and Qol-e-tut. A total of 10 samples were studied (Table 1):

1. Six fragments of sculptures preserving one or several layers. From Tepe Narenj: TN1 and TN2 (taken from Chapel 1), TN3 (from Chapel 3), and TN5 (from Chapel 4). From Qol-e-tut: QT2 and QT4 (taken from Chapel 6).
2. Two fragments of mural paintings or reliefs: TN4 (taken from Chapel 4 of Tepe Narenj) and QT1 (from Chapel 13 of Qol-e-tut).
3. Two samples taken from the walls surface of the most representative rooms preserving sculptural decoration in situ (TN6 from Chapel 4 of Tepe Narenj and QT3 taken from Chapel 13 of Qol-e-tut).

As said above, except TN6 and QT3, extracted directly from the walls surface, the sampled fragments were preserved close to their respective sculptural or mural origin, awaiting a hypothetical future restoration.

Methods

Different analytical techniques were applied depending on the morphology of the fragments recovered in Tepe Narenj and Qol-e-tut, and the questions to be answered concerning the formulation of the layers, the nature of the stucco, and the presence of organic binders.

TABLE 1 Samples analyzed, location, subsamples ID, and description.

Sample ID	Location	Subsample ID	Description
Sculpture			
TN1 (clothing fragment)	Tepe Narenj - chapel 1 (recovered from a basket deposited on the central pedestal)	TN1 a	Stucco layer (Munsell 10YR 7/3)
		TN1 b	Light brown clay-based layer (Munsell 10YR 6/3)
TN2 (possible fragment of halo with incised decoration)	Tepe Narenj - chapel 1 (recovered from a basket deposited above the stone socle of the south wall)	TN2 a	'Barbottina' layer (Munsell 10R 5/6)
		TN2 b	Reddish clay-based layer (Munsell 2.5YR 5/6)
		TN2 c	Brown clay-based layer (Munsell 10YR 7/3)
TN3 (possible internal body fragment)	Tepe Narenj - chapel 3 (placed above the legs of Sculpture 4 north)	TN3	Brown clay-based layer (Munsell 7.5YR 6/4)
TN5 (hair fragment)	Tepe Narenj - chapel 4 (recovered from a basket near the entrance door)	TN5	Stucco layer with incised curved lines (Munsell 10YR 7/3)
QT2 (clothing fragment)	Qol-e-tut - chapel 13 (recovered from a basket placed at the foot of the "colossal Buddha")	QT2_a	Pigmented layer (Munsell 2.5YR 7/6)
		QT2_b	Stucco layer (Munsell 10YR 7/3)
		QT2_c	Brown clay-based layer (Munsell 10YR 7/3)
QT4 (fragment of a toe)	Qol-e-tut - chapel 6 (recovered from foot fragments preserved next to the remains of the right foot of a Monumental Buddha)	QT4	Brown clay-based layer (Munsell 7.5 YR 5/4)
Relief and mural painting			
TN4 (relief fragment)	Tepe Narenj - chapel 4 (recovered from a basket near the entrance door)	TN4	Brown clay-based mortar (Munsell 10YR 6/3) with a
			Red polychromed surface finish
QT1 (mural painting fragment)	Qol-e-tut - chapel 13 (recovered from a basket placed at the foot of the ""Great Buddha")	QT1	Brown clay-based mortar (Munsell 10YR 6/3) with a
			Blue and red polychromed surface finish
Walls			
TN6	Tepe Narenj - chapel 4 (northern wall, originally in contact with the back of the sculptures)	TN6	Brown clay-based mortar (Munsell 10YR 6/3)
QT3	Chapel 13 Qol-e-tut (northern wall)	QT3	Brown clay-based mortar (Munsell 10YR 6/3)

Petrography

Petrographic analysis on thin section was carried out in all samples except QT4 (a fragment of a toe from the monumental feet preserved in Chapel 6 of Qol-e-tut, which, due to its importance, we did not want to destroy by embedding it in resin in order to carry out the thin section). Optical microscopy (OM) study was carried out using a Zeiss-Axioskop 40 microscope coupled with a Canon PowerShot A640 camera for the acquisition of images under polarized light. 2D qualitative visual charts were used to estimates the aggregate roundness (Boggs, 2010;

Powers, 1953), the sorting (Boggs, 2010; Jerram, 2001), and the percentages of aggregate (as volume fractions) and macroporosity (d > 1/16 mm) (Myron Best 2003; Ricci, 1980). The different layers observed in the studied fragments are indicated in Table 4; they were defined adding the letters a, b, and c to the sample's ID, to indicate the different layers from the surface inward (i.e., QT2_a corresponds to the pigmented superficial layer, QT2_b corresponds to the stucco layer, and QT2_c corresponds to the clay preparatory layer).

Mineralogy

Semiquantitative mineralogical characterization of the pulverized samples was performed on all samples by X-ray powder diffraction (XRPD) through a Bruker D8 Advance diffractometer, with Cu–Ka radiation, operating at 40 kV and 40 mA. Scans were collected in the range 3°–66° 2θ using a step interval of 0.02° 2θ with a step counting time of 0.2 s. The mineralogical phases in each X-ray powder spectrum were identified by the EVA software program (DIFFRACplus EVA) by comparing experimental peaks with PDF2 reference patterns. To discriminate the typology of clay minerals the XRPD analysis was also performed after saturating the samples with ethylene glycol at 60°C for 24 hours.

Thermal analysis

Differential scanning calorimetry and thermogravimetry (DSC/TG) were carried out on all samples using a Netzsch STA 449 C Jupiter analyzer (Netzsch-Gerätebau GmbH, Selb, Germany). The pulverized samples were heated at a rate of 10°C/min in an alumina crucible under a constant aseptic oxygen flow of 30 cm^3 min^{-1}, heating from ambient temperature to 920°C, with a heating rate of 10°C/min. Derivative thermogravimetry (DTG), derivative differential scanning calorimetry (DDSC) and endothermic peaks were obtained through the Netzsch Proteus thermal analysis software (version 4.7.0).

Chemical analysis

Microchemical analyses of the clays were carried out on samples TN2, TN4, and QT4 using an electron probe micro-analysis (EPMA; model JEOL-JXA 8230) coupled with a spectrometer EDS (model JEOL EX-94310FaL1Q - Silicon drift type (Res 129 eV) and five WDS spectrometers (XCE types) equipped with LDE, TAP, LIF and PETJ crystals. All samples were polished and carbon coated with graphite using a Quorum Q150T ES sputter coater. In depth study was performed through energy dispersion microanalysis by scanning electron microscope (SEM-EDS), using an Ultra High-Resolution SEM (UHR-SEM)–ZEISS CrossBeam 350, equipped with an EDS–EDAX OCTANE Elite Plus, Silicon drift type spectrometer (instrumental acquisition conditions: HV: 15 keV; Probe current: 100 pA; working distance: 11 mm, Take off: 40°, Time: 30 sec.).

Raman spectroscopy, used to verify some of the details observed under optical microscope and to study the reddish layer of TN2 (TN2_b) and the pigmented layers of QT1 and QT2, was carried out through a Thermo Fisher DXR Raman microscope, equipped with OMNICxi Raman Imaging software 1.0, an objective 50×, a grating of 900 ln/mm (FWHM) and an EMCCD. The 532.0-nm line (solid state laser) was used at an incident power output ranging from 1.8 to 7 mW. The spatial resolution of the laser beam is 3–5 μm about.

To understand if an organic binder was present in the samples, epifluorescence and gas chromatography coupled with mass spectrometry were carried out on specific samples:

- Thin sections of TN1, TN2, and TN5 were examined through epifluorescence. The epifluorescence was induced by an Hg vapor lamp linked to a Zeiss Axioplan II imaging microscope equipped with high performance wide band pass filters (BP 436/10 nm/LP 470 nm for green light; BP 450–490 nm/LP 520 nm for yellow light).
- A preliminary organic residue analysis was carried out only on subsamples of QT2 (a fragment of the colossal polychromed Buddha preserved in Chapel 13 of Qol-e–e-tut presenting several layers). To perform it, samples from QT2_c (lab. M1, clay), QT2_b (lab. M2, white area), and QT2_a (lab. M3, pink area) were analyzed. Samples were mechanically cleaned before subsampling and powder was recovered with a scalpel. Powders were extracted following two extraction methods: (i) the direct methanolic extraction (Correa-Ascencio & Evershed, 2014) and (ii) the alkaline extraction (Pecci et al., 2013, 2020). Although the extraction protocol suggests to analyze 2 g for extraction (i.) and 1 g for extraction (ii), due to the need of preservation of the samples, extraction (i) was applied only to respectively 1 g (QT2_c-clay), 0.15 g (QT2_b -white area) and 0.03 g (QT2_a -pink area); whereas extraction (ii) was applied only to 0.5 g (M1), 0.17 g (M2) and 0.11 g (M3). 50 μl of internal standard (n-hexatriacontane) was added to all the samples. The extracts were derivatized with N, O-bis (trimethylsilyl)trifluoroacetamide (BSTFA) and analyzed with gas chromatography coupled to mass spectrometry (GC–MS). For the analyses, a Thermo Scientific TS GC ultra-gas chromatograph was used, with a 30 m silica capillary column and a thickness of 0.25 μm coupled with a Thermo Scientific ITQ 900 mass spectrometer operated in electronic ionization (70 eV). The mass range was m/z 40–650.

RESULTS

As previously mentioned, the modeling pastes of the monumental terracruda sculptures from Tepe Narenj and Qol-e-tut show one or several layers, generally composed of a clay-based paste, sometimes covered with a thin final coat of stucco or 'barbottina' layer and, in one case, a finishing pigmented layer with traces of color.

Roundness (Boggs, 2010; Powers, 1953): SA: subangular.

Sorting (Boggs, 2010; Jerram, 2001): MS: moderately sorted; MWS: moderately well sorted; PS: poorly sorted. Mineralogical phases: Act: actinolite; Alm: almandine; Amp: amphibole, Anh: anhydrite, Bt: biotite; Cal: calcite, Chl: chlorite; Chr: chrysotile; Ep: epidote, FeAct: ferro-actinolite; Ferrihy: ferrihydrite; Gyp: gypsum; Ill: illite; Lz: lizardite; Mc: microcline; Mon: montmorillonite; Ms: muscovite; Om: opaque mineral; Or: orthoclase; Pl: plagioclase, Qtz: quartz.

Compositional characterization of the modeling pastes

According to the mineralogical and petrographic analysis, in all the samples studied, the clay layers of the pastes have a similar aggregate composition (Table 2) with the presence of metamorphic rocks fragments, such as phyllite (Figure 2a) and quartzite (Figure 2b), and carbonate rocks, such as microsparite, cryptocrystalline limestone (Figure 2c) and traces of calcarenite (only in TN6). The mineralogical phases common in almost all samples are quartz, biotite, orthoclase, muscovite (Figure 2d), amphiboles (in particular actinolite–Figure 2e), calcite (Figure 2d), plagioclase, chlorite, microcline (Figure 2f), and opaque minerals (Table 2). In some samples traces of epidote (in TN1 and QT3), traces of ferrihydrite (in TN1 and TN3), and traces of lizardite (in TN4) are also visible. The clay used in these layers is mainly composed of illite and montmorillonite, identified after the treatment with ethylene glycol (Figure 3).

TABLE 2 Results of petrographic and mineralogic analyses.

Sample	Layers	Typology	Binder color	Max aggregate size (mm)	Mean aggregate size (mm)	Wentworth size	Roundness	Sorting
QT1	–	Clay layer	Brown	2.82	1.09	Very coarse sand	SA	MS
QT2	QT2_a	Pigmented layer	Gray	Layer with a thickness of 0.5 mm. Its aggregate is not solvable through optical microsocopy				
	QT2_b	Stucco layer	Gray	Layer with a thickness of 2 mm and an oriented high porosity due to voids left by the fibers				
	QT2_c	Clay layer	Brown	1.24	0.88	Coarse sand	SA	MWS
QT3	–	Clay layer	Brown	3.98	0.70	Coarse sand	SA	PS
TN1	TN1_a	Clay layer	Gray	0.68	0.18	Fine sand	SA	MWS
	TN1_b	Clay layer	Ligth brown	1.73	0.77	Coarse sand	SA	MWS
TN2	TN2_a	"Barbottina" layer (clay slip)	Brown	–	–	–	–	–
	TN2_b	Clay layer	Reddish	1.19	0.53	Coarse sand	SA	MWS
	TN2_c	Clay layer	Brown	0.87	0.26	Medium sand	SA	MWS
TN3	–	Clay layer	Brown	1.73	0.45	Medium sand	SA	MWS
TN4	–	Clay layer	Brown	2.32	0.56	Coarse sand	SA	MS
TN5	–	Stucco layer	Gray	0.21	0.09	Very fine sand	SA	MWS
TN6	–	Clay layer	Brown	7.50	1.39	Very coarse sand	SA	PS

TABLE 2 (Continued)

Sample	% aggregate (size >1/16 mm)	% binder (size <1/16 mm)	% macro porosity (size >0.05 mm)	Aggregate/ binder ratio	Mineralogical phases by OM, XRPD, DSC/TG, and Raman spectroscopy	Rock fragments	Other
QT1	20	68	12	0.3	Qtz, Bt, Or, Mc, Ms, Amp (Act), Cal, Pl, Chl, Om, ill, Mon	Metamorphic fragments, micritic limestone	Recristallized calcite
QT2	Layer with a thickness of 0.5 mm. Its aggregate is not solvable through optical microsocopy						
	Layer with a thickness of 2 mm and an oriented high porosity due to voids left by the fibers				Gy, Qtz (tr)	–	–
	45	47.5	7.5	0.9	Qtz, Bt, Pl, Or, Ms, Mc, Amp (FeAct), Cal, Alm, Chl, ill, Mon, Om	Metamorphic fragments, micritic limestone	Oriented porosity probably due to the presence of fibers
QT3	30	50	20	0.6	Qtz, Bt, Amp (Act), Pl, Or, Ms, Ep, Cal, Chl, Om, Ill, Mon	Metamorphic fragments, micritic limestone	–
TN1	3	77	20	0.04	Gy, Qtz, Or, Pl, Cal, Om	–	–
	40	50	10	0.8	Qtz, Bt, Amp (Act), Pl, Or, Mc, Ms, Om, Cal, Gyp, Ep, Chl, Ferrihy, ill, Mon	Metamorphic fragments, micritic and criptocristalline limestone	Traces of oriented porosity probably due to the presence of fibers
TN2	–	–	–	–	Traces of Bt, Ms, and Qtz	–	–
	45	50	5	0.9	Qtz, Bt, Pl, Or, Ms, Cal, Amp (Act), Chr, Chl, Om, Ill, Mon	Metamorphic fragments, micritic limestone	–
	10	82.5	7.5	0.1	Qtz, Bt, Amp (Act), Ms, Chl, Om, Ill, Mon	Metamorphic fragments (tr)	–
TN3	15	60	25	0.3	Qtz, Bt, Pl, Or, Amp (Act), Ms, Cal, Chl, Gyp, Om, Ill, Mon, Ferrihy	Metamorphic fragments, micritic limestone	Oriented porosity probably due to the presence of fibers
TN4	20	68	12	0.3	Qtz, Bt, Pl, Or, Amp (Act), Ms, Cal, Chl, Om, Lz, ill, Mon	Metamorphic fragments, micritic limestone	–
TN5	2.5	87.5	10	0.03	Gyp, Anh, Qzt, Amp (Act), Bt, Ms, Om	–	–
TN6	45	25	30	1.8	Qtz, Bt, Pl, Or, Amp (Act), Ms, Cal, Chl, Om, Ill, Mon	Metamorphic fragments, micritic limestone, calcarenite	–

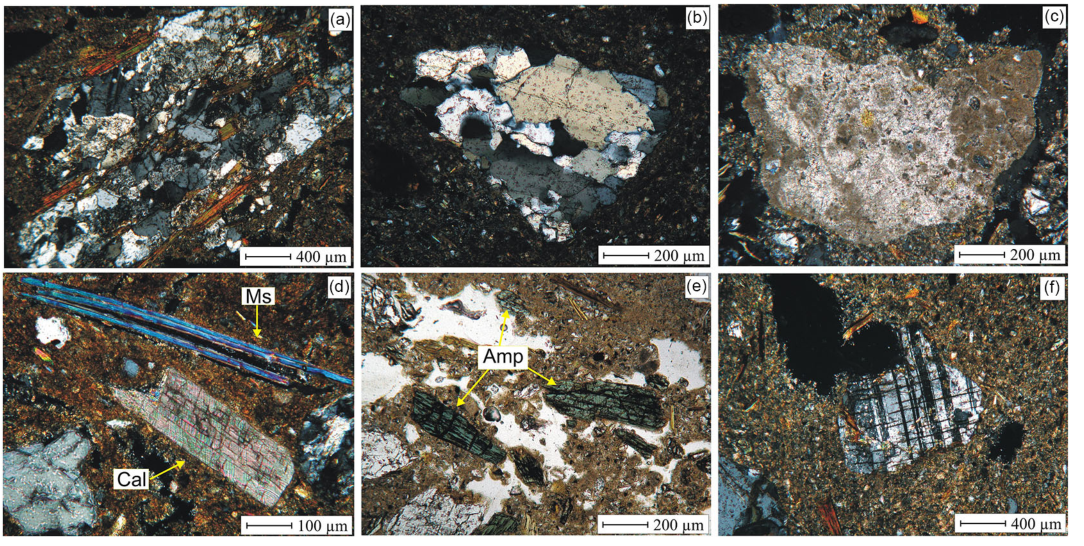

FIGURE 2 Microphotographs in thin section under crossed nicols. (a) Phyllite in sample QT3. (b) Quartzite in sample TN4. (c) Cryptocrystalline limestone in TN1. (d) Muscovite (Ms) and calcite (Cal) in TN2. (e) Amphiboles (Amp) in QT3. (f) Microcline in QT1.

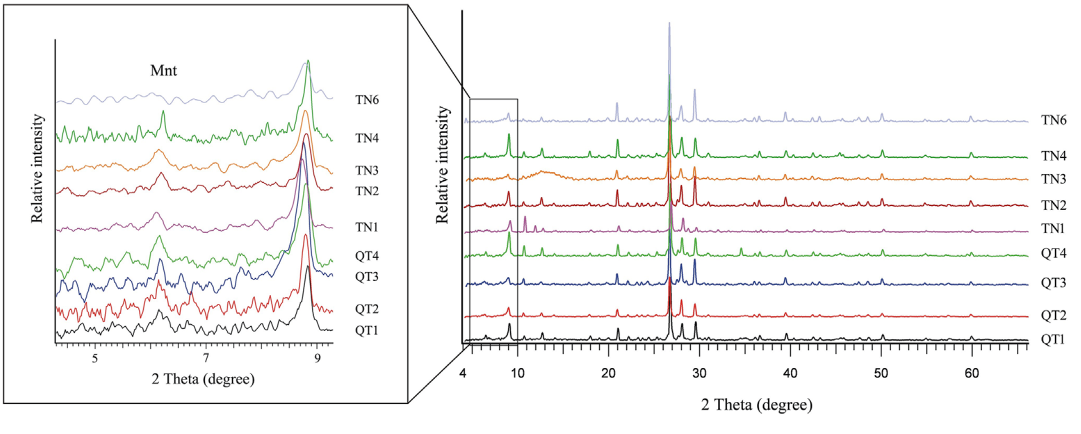

FIGURE 3 Powder X-ray diffraction patterns from untreated clay samples (on the right) and samples after ethylene-glycol treatment (on the left) Mnt: montmorillonite.

Micromorphological observations and microanalysis by electron probe performed on samples confirmed the phyllosilicate origin (clays and mica) of the matrix (Figure 4a). The micro-nanomorphological study did not reveal skeletal remains of marine fossils and microfossils. No planktonic microforaminifera, calcareous nanofossils, radiolarians, or diatoms, whose presence is associated with fine sediments of pelagic origin, were found. On the contrary, the clay matrix is rich in vascular plant remains and in particular epidermis fragments (Figure 4b–d) and pollen (Figure 4e).

The absence of fossils of marine origin and the presence of numerous remains of vascular plants, associated with rare, rounded corpuscles, tentatively interpreted as charophytes-like remains (Figure 4f), suggest a deposition of the clays in a low-hydrodynamic system, strongly influenced by terrestrial input (i.e., a paludal/lacustrine environment). These remains could

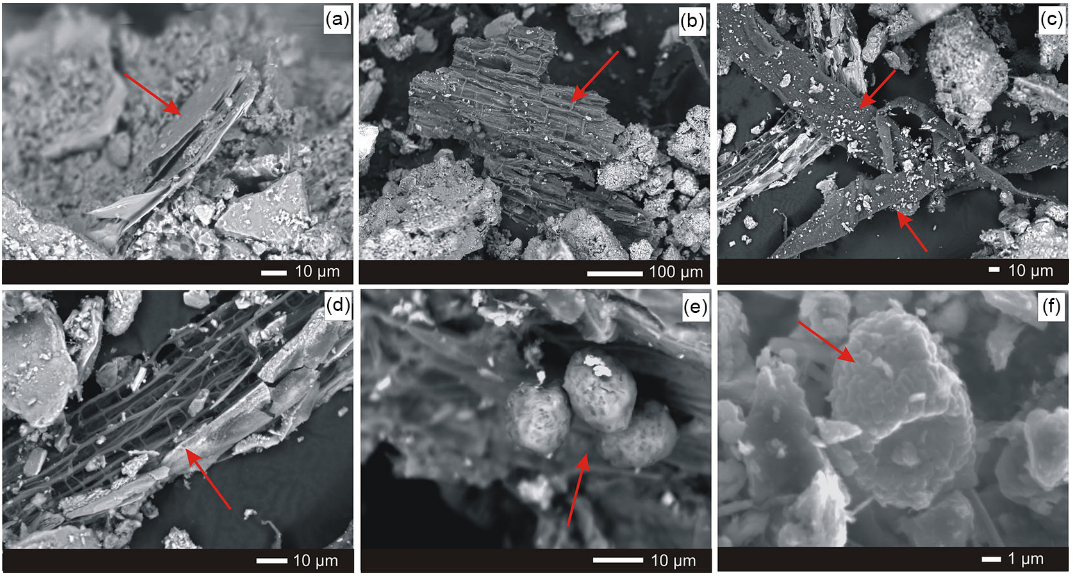

FIGURE 4 Microphoto by EMPA. (a) Particular of sample TN2 in which the phyllosilicate origin of the matrix is evident. (b–d) Cuticles in sample TN4. (e) Pollen in sample TN4. (f) Oogonia in sample QT4.

represent fragments of plants originally present in the clay at the moment of mining or have been added later to the clay while being prepared for its different uses. In the first case, their presence, coupled with the absence of marine remains, would suggest a terrestrial/lacustrine origin of the clays that could have been mined in the lake Qol-e-Hashmat Khan, located at the foot of both sites. This hypothesis will be verified in future studies through the mineralogical, paleontological, and geochemical characterization of clay samples collected in the presumed area of provenance. The geological literature of the area is scant and the only clay sediments reported are dolomitic in composition, with a high content of montmorillonite (Pias, 1976). These clay outcrops near the microbreccias of the "formations rubéfiées," not far from Kabul. However, even if they are barren in microfossils, the absence of dolomite in the archaeological samples makes the use of dolomite clays unlikely in the manufacturing of the sculptures.

Although the mineralogical-petrographic data indicate a very similar composition and, consequently, a common extraction quarry, it is possible to observe differences among the samples related to the diverse types of architectural elements of which they were a part, suggesting a different processing of the clay-based pastes depending on the items to be produced.

The sculptures

The sculpture samples (TN1, TN2, TN3, TN5, QT2, and QT4) show some differences and some similarities. In particular:

- Samples TN1 and QT2 are very similar, both of them are clothing fragments modelled with a clayey mortar and finished respectively with a layer of white stucco. In sample QT2 a superficial thin layer of about 0.5 mm (QT2_a) is also visible, which corresponds to the pigmented surface with a pink color (Munsell 2.5YR 7/6) (Figure 5a). The stucco layers, identified as TN1_a, and QT2_b, show a grayish binder (Munsell 10YR 7/3) made of gypsum (identified by XRPD and EDS analyses) and are characterized by high porosity (Figure 5b) due to the

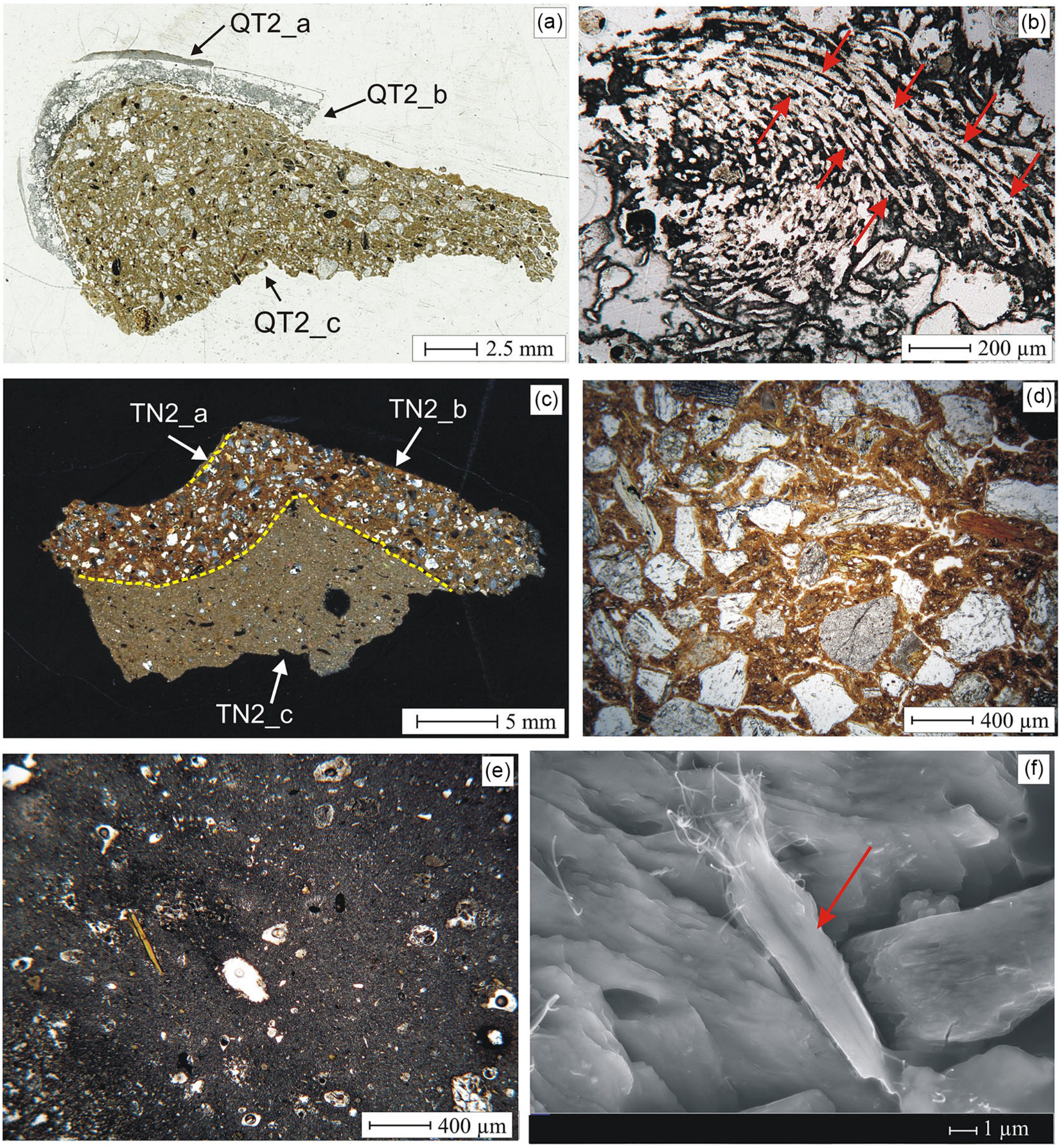

FIGURE 5 (a) Different layers in QT2, scan of the thin section under parallel nicols. (b) Stucco layer in TN1_a, arrows indicate the voids left by the fibers, micro photo in thin section under parallel nicols. (c) Different layer in TN2, scan of thin section under crossed nicols. (d) TN2_b layer where the red color of the clay is evident, micro photo in thin section under parallel nicols. (e) Sample TN5, micro photo in thin section under parallel nicols. (f) SEM image with particular of a fiber in TN5.

voids left by fibers or herbaceous matter (for the characterization of these layers see paragraph 6.2). The underlying layers (TN1_b and QT2_c) are composed of a coarse sand aggregate (Wentworth, 1922), moderately well sorted (MWS) (Boggs, 2010; Jerram, 2001) with a very similar aggregate/binder ratio (respectively 0.9 and 0.8). Oriented porosity is also visible, in particular in QT2_c, where the enrichment of phytoliths of wood morphotypes, identified during previous analyses, could be related to the possible contact of this fragment with internal parts or strata of the sculpture, as suggested by the negative herbaceous imprints preserved on its internal surface (López-Prat, Lancelotti, et al., 2022). The presence of bast fibers and herbaceous matter in the samples added to the clay mixtures was also documented by López-Prat, Lancelotti, et al. (2022). It should also be noted that the macroscopic photographs of the stucco from QT2 (Figure 6) seem to indicate the remains of fabric between the stucco layer and the underlying earthen mortar, something that could not be fully clarified by the study of thin sections and that needs to be studied more accurately in the future.

- Sample TN3, which to the naked eye appeared to show more than one layer, in thin sections shows only one clayey layer, without a stucco surface. However, its morphology and composition are very similar to TN1_b and QT2_c, with the presence of an oriented high porosity (25%) due to the remains of herbaceous matter. In addition, TN1_b and TN3 are the only samples that contain ferrihydrite (identified by XRPD) and gypsum, visible on thin section and confirmed by XRPD. The gypsum, in the form of angular crystals inside the porosity, corresponds to a recrystallized secondary gypsum.
- Sample TN2 is totally different from the previous samples. It is the only sculptural fragment in which two clayey layers are distinguishable in thin section (TN2_b and TN2_c), with a third thin superficial layer (TN2_a) only partially preserved (Figure 5c). TN2_a seems to correspond to a red (Munsell 10YR 5/6) 'barbottina' layer (clay slip), composed of a brown binder with traces of biotite, muscovite, and quartz. The layer TN2_b shows a reddish binder (Figure 5d) composed of hematite, identified by Raman spectroscopy. Most likely, hematite was intentionally added in the mixture to give the red color, in fact the composition of the clay in all samples is the same (see Compositional characterizarion of the modelling pastes, Figure 3). TN2_b layer shows a very high percentage of aggregate (45%) of coarse size (Wentworth, 1922). On the contrary, the underlying layer (TN2_c) shows a much lower percentage of aggregate (10%) and a finer grain size (medium sand).
- TN5 corresponds to a fragment of 'stucco', morphologically identified as part of the hairdo of a sculpture. However, it is completely different from the stucco layer of sample TN1 and QT2. It is composed of a greyish binder (Munsell 10YR 7/3) (Figure 5e) made of gypsum and anhydrite, identified by XRPD, with a very low percentage of aggregate (2.5%) that is very fine (Wentworth, 1922) and moderately well sorted (Boggs, 2010; Jerram, 2001) (for the characterization of this layer see paragraph 6.2). Although an oriented porosity is not visible, traces of fibers were identified by SEM-EDS (Figure 5f).

FIGURE 6 Remains and imprints of a fabric between the stucco layer and the underlying earthen mortar in sample QT2. Left: OM Image 8× LEICA-EZ4W. Right: macroscopic view of a fragment of the internal part of QT2.

- QT4 corresponds to a toe fragment 35–40 mm in diameter. To the naked eye it appears to be composed of a single layer of a very hard and compact brown clay (Munsell 7.5 YR 5/4) with some mineral inclusions. Due to its relevance (fragment of a toe), no thin section could be done, and the sample was only analysed by XRPD and EPMA to characterize the clays.

The mural paintings and reliefs samples

Samples QT1 and TN4 are composed by only one layer with a polychromed surface. They show the same aggregate/binder ratio, the same density porosity (12%), and are the unique fragments with a moderate sorting degree (MS) (Boggs, 2010; Jerram, 2001). These data, together with an enrichment in chaff phytoliths (TN4) and nettle/ramie fibers (QT1) (López-Prat, Lancelotti, et al., 2022), seem to confirm that these are not sculpture samples but wall finishes associated with bas-relief murals (in the case of TN4, with volume-forms obtained through the addition of herbaceous matter) or mural painting (QT1) without an enrichment of phytoliths but a clear addition of fibers, which could be due to the need to produce smooth surfaces with the necessary performance for optimal drying to carry out the paintings.

The wall samples

Samples TN6 and QT3 are fragments extracted respectively from the walls of Chapels 4 and 13 of Tepe Narenj and Qol-e-tut respectively. They show a very coarse sand and a coarse sand aggregate (Wentworth, 1922), a high porosity variable from 20% (in QT3) to 30% (in TN6), and are the only samples with a poor sorting degree (PS) (Boggs, 2010; Jerram, 2001). These data contrast with the clayey mortars of the rest of the studied samples, which indicate a moderately well-sorting degree (MWS), except two (QT1 and TN4, mural painting and bas-relief respectively), in which it is moderate (MS). These data clearly identify TN6 and QT3 with less processed clayey pastes compared to the rest of the fragments studied.

The nature of the 'stucco' layers

As mentioned above, the nature of the 'stucco' layers is one of the common inquiries found in literature concerning archaeological clay-based sculptures. Stucco was present in fragments TN1 (TN1_a), TN5 and QT2 (QT2_b), and its main mineral component has been identified as gypsum with an oriented and elongated porosity due to the voids left by fibers (Figure 5b). SEM-EDS analysis was performed on the stucco layer of sample TN1 and on sample TN5 to clarify whether the gypsum was cooked or if it was used raw, which means extracted from the quarry, crushed, and potentially mixed with organic matter as observed nowadays in West Bengal and mentioned in Sanskrit literature in connection with the grinding of *sarkaras* (López-Prat et al., 2021; Varma, 1970).

In layer TN1_a (Figure 7a) and in sample TN5 (Figure 7b, yellow arrow), the analysis highlighted the presence of pure microcrystalline gypsum, with very angular crystals, homogeneous in size. In both samples, the angularity of the crystals seems to indicate that the gypsum was not cooked, but it was taken from the quarry and grinded. As shown in Figure 7b, in sample TN5, inside the gypsum crystals (yellow arrows), some amorphous areas (red arrows) are visible, where SEM-EDS analysis revealed a high carbon content that indicates the presence of organic matter. In sample TN5, XRPD analysis revealed the presence of anhydrite (Table 2), which is naturally associated to the gypsum in the evaporitic deposits and could indicate a different provenance quarry, compared to TN1 sample.

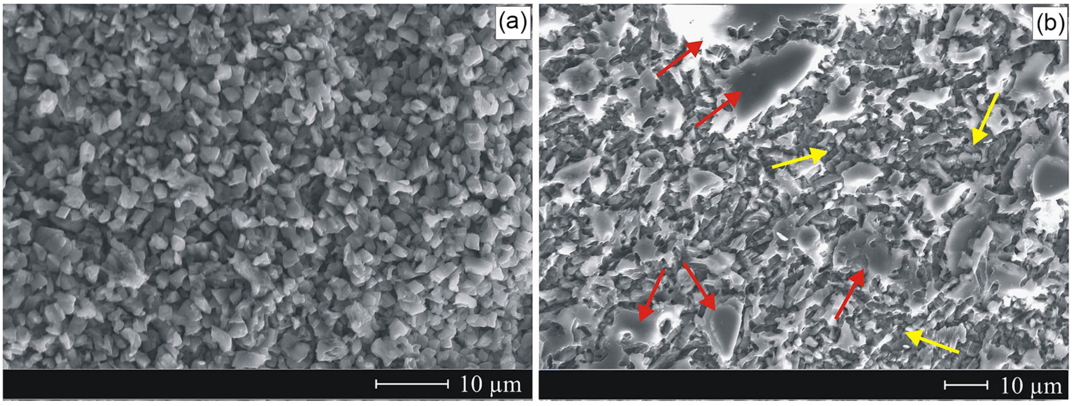

FIGURE 7 Microphoto by EMPA. (a) Crushed pure gypsum in TN1_a. (b) Crushed gypsum in TN5 (yellow arrows) and amorphous areas (red arrows) corresponding to the organic matter.

To confirm the possible presence of organic matter, some sculpture fragments clearly preserving superficial or stucco layers (TN1, TN2, TN5) were investigated through epifluorescence microscopy. Organic residues and Mn^{2+} appear to be the most abundant and important activators of fluorescence in geological materials (Neuweiler & Reitner, 1995; Russo et al., 1997). Organically activated luminescence is interpreted to be caused mainly by aromatic and certain conjugated organic molecules. In the present study, the absence of inorganic activators (Mn^{2+}) confirms the attribution of the epifluorescence to biomolecules related to organic material. Therefore, it is possible to understand that an organic binder was utilized in the stucco plasters and probably in the earthen mortars of the terracruda sculptures.

In particular, the analysis indicated the abundance of organic binder in the stucco layer of sample TN1 (Figure 8a) and in sample TN5 (Figure 8b), where the epifluorescence phenomenon is clearly visible. However, the epifluorescence can also be observed in the clay layers of sample TN2 (Figure 8c) (TN2_b and TN2_c) and, in a lesser amount, in the clay layer of sample TN1 (TN1_b) (Figure 8d).

To clarify the nature of the organic matter, preliminary analysis by GC–MS was performed on three samples recovered from the different layers of QT2, distinguishable at the macroscopic and microscopic level: QT2_c corresponding to the clay, QT2_b corresponding to the white layer, and QT2_a corresponding to the pink polychrome layer.

Before discussing the results, it is important to recall that powdered samples analyzed differ in quantity, while the same quantity of IS was added to each of the three samples and that the extraction protocol suggests analyzing 2 g for extraction (i.) and 1 g for the alkaline extraction (ii.), whereas the quantities analyzed are much lower.

Residues are scarce, most likely due to the low amount of sample analyzed and/or to the scarcity or poor preservation of organic matter in the samples. However, the extractions revealed the presence of different compounds (Table 3, Figure 9).

The presence of phthalates (dots in Figure 9) is due to the conservation of the samples in plastic bags.

Samples QT2_b and QT2_a have not methylated properly, probably due to the carbonated nature of the analyzed layer. This is consistent with the presence of gypsum in the two layers. However, the second derivatization with BSTFA was allowed to display trimethylsilylated fatty acids (FAs) (in the figure $C_{n:0}$TMS). In extract i. of the three samples (Figure 9), the main trimethylsilylated FAs identified were palmitic ($C_{16:0}$), oleic ($C_{18:1}$) and stearic ($C_{18:0}$) acids. Samples QT2_c and in a lesser extent QT2_b display a higher concentration of fatty acids, while sample QT2_a has a very low concentration, probably due to the small amount of powder analyzed.

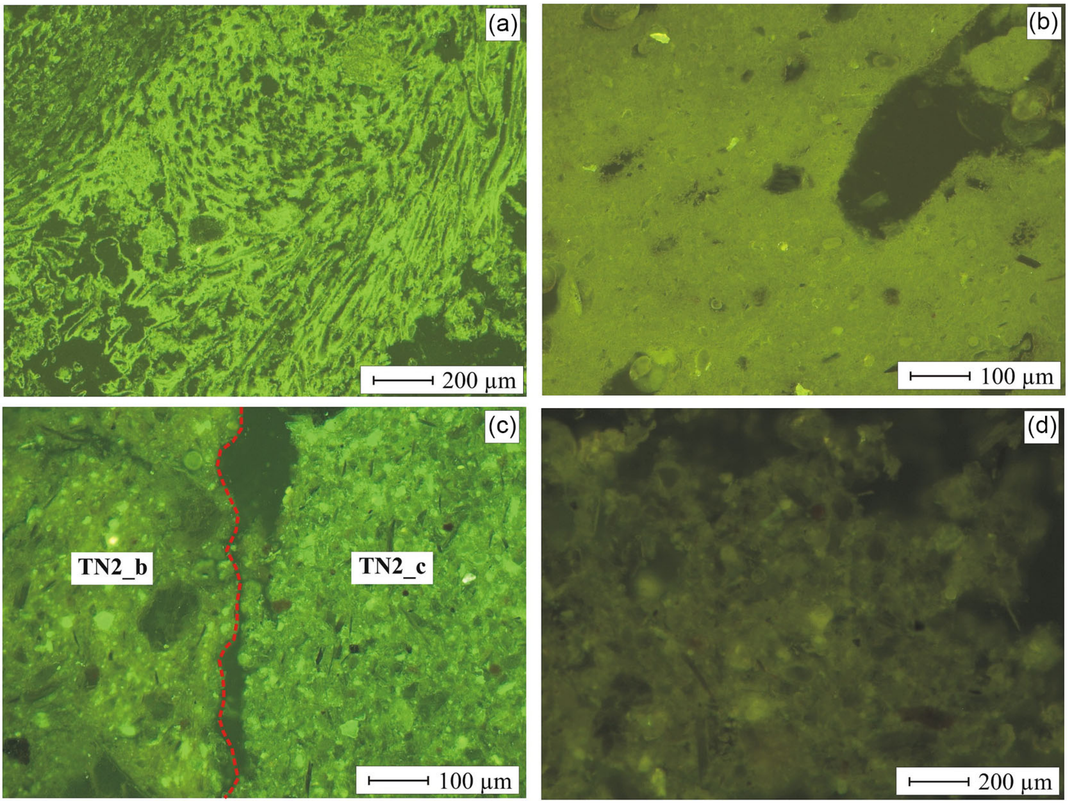

FIGURE 8 Microphotographs in thin section under epifluorescence microscopy. (a) Stucco layer TN1_a. (b) Sample TN5. (c) Layers b and c in sample TN2. (d) Clay layer TN1_b.

TABLE 3 List of the main components for each sample (FA = fatty acid; $C_{18:0}$ = stearic acid; $C_{18:1}$ = oleic acid; $C_{16:0}$ = palmitic acid; S_{27} = cholesterol; βS = β-sitosterol, TA = tartaric acid; N = none; Y = yes).

Sample ID		Sample analyzed Ext i (g)	Sample analyzed Ext ii (g)	Main FAs in order of decreasing concentration	S_{27}	βS	TA
QT2_c	M1 Clay	10,203	0.5076	$C_{16:0}$ $C_{18:1}$ $C_{16:1}$ $C_{18:0.}$ $C_{14:0}$	Y	Y	-
QT2_b	M2 White layer	0.1591	0.1714	$C_{16:0}$ $C_{18:1}$ $C_{18:0}$	Y	N	-
QT2_a	M3 Pink layer	0.0320	0.1129	Traces of $C_{16:0}$ $C_{18:1}$ $C_{18:0}$	Y	N	-

The relative abundance of fatty acids suggests the presence of plant origin products, although β-sitosterol, generally present in plant products, was identified only in QT2_c. Cholesterol (S_{27}) was identified in all three samples, and its high content in QT2_c seems to suggest that it derives from contamination (Hammann et al., 2018). The organic residues identified would be related to the need for an organic binder to amalgamate the ground gypsum in the case of the stucco layer and to add some particularity to the behavior of the clay-based pastes.

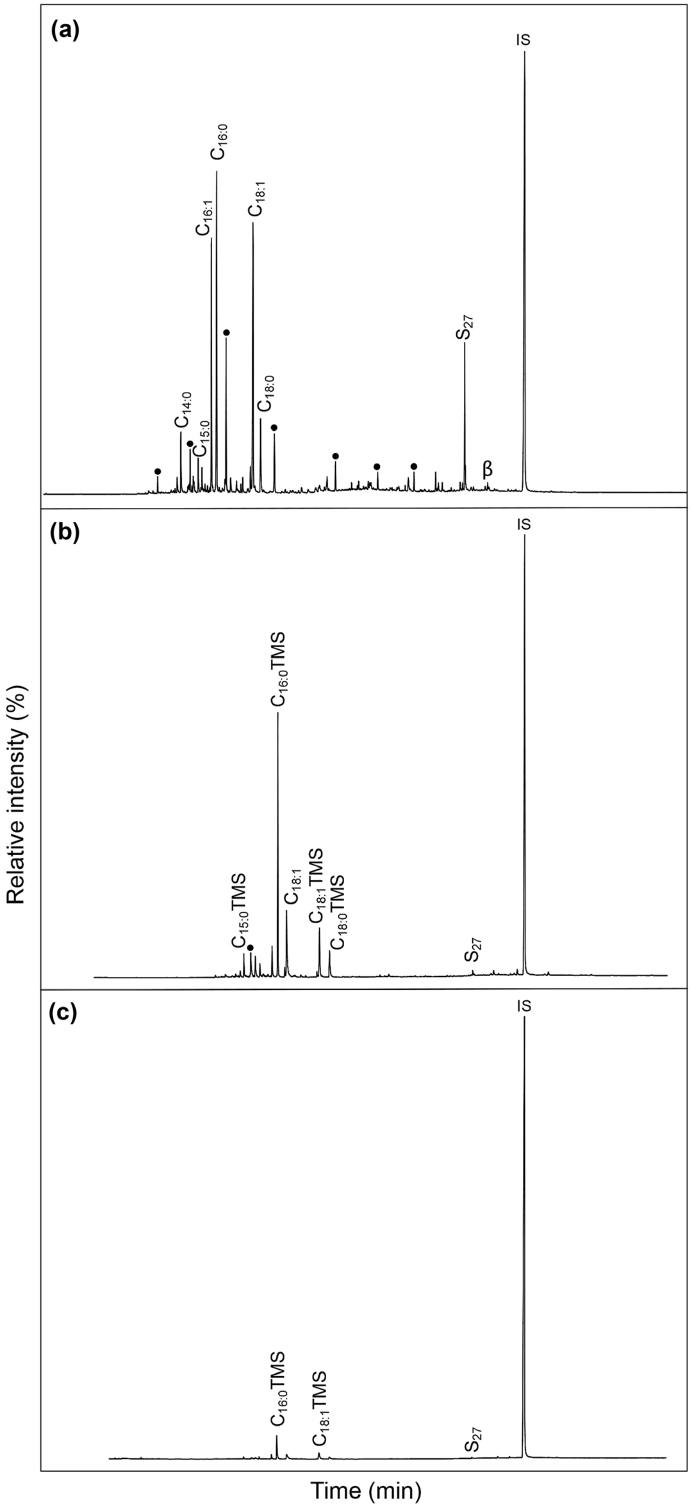

FIGURE 9 Partial gas chromatograms from exctracts (i) of samples (a) QT2_c, (b) QT2_b, and (c) QT2_a. [Cn:0 TMS = trimethylsilylated fatty acids with a specific number (n) of carbons, S_{27} = cholesterol, β = β-sitosterol, dots = phthalates, and IS = internal standard].

No Pinaceae products (resin or pitch) were identified in any of the extracts of the three samples, therefore no resin/pitch from Pinaceae was used as a binder in the preparation of the different layers. Extraction ii. was developed in order to identify wine residues in archaeological samples and in particular to identify tartaric acid (Pecci et al., 2013, 2020). Although it is generally considered the marker for grape derivatives, tartaric acid is also present in tamarind, which today is used in West Bengal in the making of the stucco layers of terracruda sculptures. As no tartaric acid was identified in extract ii., the results of the analyses indicate that this substance was not used in the preparation of any of the layers of QT2.

Pigments characterization

To determine the nature of the pigmented layers visible on samples QT1 (mural painting fragment) and QT2 (sculpture fragment), Raman spectroscopy analysis was performed. The colors visible on the surface of the two samples are blue and red for sample QT1 and pink (light red) for QT2 (see Table 1).

As shown in Figure 10a, in sample QT1 Raman spectroscopy highlighted the presence of lazurite (Figure 10a), and consequently of lapis lazuli, for the blue pigment, and the presence of hematite for the red pigment (Figure 10b), both of them dispersed in a calcitic binder (Figure 10c).

The pink pigment present on the surface of sample QT2 is also composed of hematite, but in this case, it is dispersed in a gypsum-based binder. Indeed, the Raman spectrum obtained is given by the superimposition of the hematite and gypsum signals (Figure 10d).

DISCUSSION

Notwithstanding the similarities in mineral-petrographic composition of different clay-based pastes studied, some relevant differences in processing can be observed among the samples, mainly liked to their different typology: sculpture, mural paintings, reliefs, or walls. Although the fragments of mural painting, reliefs, and walls show a single type of clay-based paste and no distinguishable layers, the sculpture samples clearly show a superimposition of layers with a different composition and processing of the pastes.

If we focus only on sculpture pastes of a clayey nature (TN1_b, TN2_b, TN2_c, TN3, and QT2_c), it is possible to highlight some differences linked to the percentage of aggregate and clay

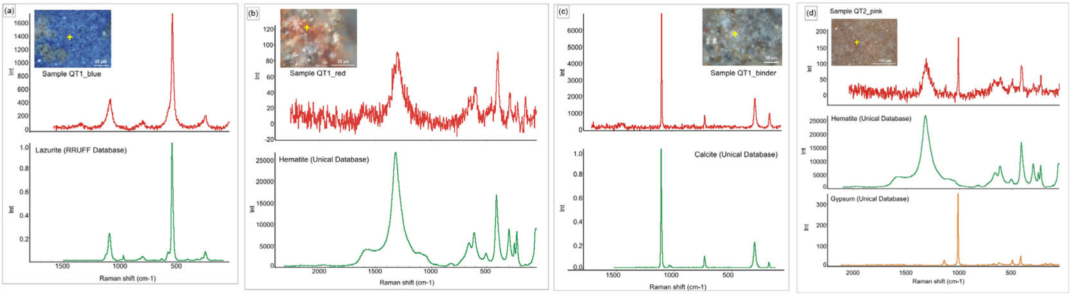

FIGURE 10 (a) Raman spectra of the blue pigment analyzed in sample QT1 and of lazurite present in the RRUFF database (RRUFF ID: R040023). (b) Raman spectra of the red pigment analyzed in sample QT1 and of hematite present in the Unical database. (c) Raman spectra of the QT1 binder and of calcite present in the Unical database. (d) Raman spectrum of the red pigment analyzed in sample QT2 and comparison with the hematite and gypsum spectra present in the Unical database.

binder that would lead to dividing them into two groups: (i) pastes with abundance of aggregate (about 40–45%) in samples TN1_b, TN2_b, and QT2_c; and (ii) pastes with higher presence of binder (aggregate about 10–15%) for samples TN2_c and TN3. In this sense, it is interesting that ethnographic studies carried out in West Bengal on contemporary production of terracruda sculptures produced in a traditional way (López-Prat, Agostino, et al., 2022; López-Prat, Lancelotti, et al., 2022) suggest that there are differences in the production process. The internal layers are made with *etel-mati* (which means sticky clay in Bengali), a more plastic and adhesive clay-based paste where the binder fraction is prevailing, mixed with a greater quantity of herbaceous matter (straw, husk) to give volume to the sculpture. The upper layers are made with *bele-mati* (which means sandy clay in Bengali), where the aggregate fraction increases to facilitate the modeling of details and to minimize the cracks during the drying process, sometimes with addition of jute fibers or a total absence of vegetable component, to facilitate a smooth finish. Although very distant in time and geographical area, it is remarkable to suggest that a similar pattern has been used to make the different layers of the archaeological sculptures sampled from Tepe Narenj and Qol-e-tut. It is particularly noteworthy that TN2_c and TN3 (where the binding fraction is prevalent) seem to belong to internal layers of sculptures, whereas TN1_b, TN2b, and QT2_c (where the aggregate fraction is higher) correspond to superficial layers. This seems concordant to the idea offered by the literature (Blänsdorf & Melzl, 2009; Klimburg-Salter, 2018; Verardi, 1983), which usually define the internal layers as 'coarser,' a perception that could be derived by the use of abundant herbaceous matter (straw, husk) in the inner layers to give volume to the sculptures, which in the case of sculptural fragments of Tepe Narenj and Qol-e-tut was confirmed by previous analysis of phytoliths and fibers in archaeological samples (López-Prat, Lancelotti, et al., 2022), and it is also documented in the current Bengali tradition (López-Prat et al., 2021). These different types of clay could correspond also to the soils mentioned in Sanskrit literature and translated by Varma as 'sandy soil' *(jangala*) and 'moist soil' *(anupa*). According to his study of agamic literature, the inner layers are assembled with the wettest type of clay or *anupa*, and the outer with the sandier clay or *jangala* (Varma, 1970, p. 87).

The use of a more clayey paste for the inner layers and a sandier clay for the outer layers is also documented in other terracruda sculptures when petrographic analyses have been carried out on the modeling pastes. This would be the case of the monumental terracruda sculptures from Old Nisa, in Turkmenistan (Chiari, 1993); Bamiyan, in Afghanistan (Blänsdorf & Melzl, 2009); Nako, in the Indian Himalayas (Bayerová et al., 2010); and Guanyin, in China (Zhao, 2014).

As for the finishing coats of the samples studied from Tepe Narenj and Qol-e-tut, their production clearly shows different procedures. Thus, the mineralogical-petrographic analyses carried out on fragments associated with polychrome mural decorations (QT1 and TN4) do not show any preparatory or stucco layer prior to the application of the color. However, in the case of fragments linked to sculptures, two types of finishes have been identified as 'stucco' (TN1, TN5, and QT2) and 'barbotine' (TN2_a).

The barbotine coating of TN2 (TN2_a) could be associated with the specificity of the fragment, an example of a stylistic current that favors this tonality in the sculpture finishes that, according to archaeologists, dates to a late period (7th- 8th cent. AD) of the Afghan Buddhist production (Forgione, 2019; Paiman, 2018). From this fragment, also highlights the total absence of plant micro-remains and a very low presence of fibers in TN2_b compared to any other clayey paste of any other sample studied (López-Prat, Lancelotti, et al., 2022), which translates into a very low porosity of the mortar (5%). These features, together with the high amount of aggregate and the high epifluorescence phenomenon observed in TN2_b, could be responsible for the exceptionally hard nature of this clay-based paste.

On the contrary, the electron probe microscopy and epifluorescence performed on samples of Tepe Narenj and Qol-e-tut presenting a finishing coat of stucco confirm the use of raw gypsum (calcium sulfate dihydrate) grinded and mixed with organic binders, a procedure mentioned by Sanskrit texts (Varma, 1970) and nowadays practiced in West Bengal (López-Prat et al., 2021). This layer would act as a primer, applied at the end of the modeling process to prepare the sculpture for polychromies. This particular use of gypsum could also fulfill a material requirement because the use of hemihydrate calcium sulfate (the so-called plaster of Paris) on air-dried clay would cause a rapid loss of water from cooked gypsum and the consequent appearance of multiple craquelures on this material. It is worth mentioning at this point Chiari's (1993) examinations of monumental sculptures in terracruda from Old Nisa, when analyzing the stucco layer, identifies the mineral components of the white stucco 'as finely ground quartz mixed with kaolin and a small amount of calcite which is not sufficient to suggest the use of a lime mortar,' something that would be aligned with what Varma pointed out when translating the Sanskrit texts (Varma, 1970).

The application of a finishing made of stucco could imply the addition of fabric, as stated in some archaeological descriptions (Barthoux, 1930; Bernard, 1969; Paiman, 2010; Tarzi, 1986; Verardi, 1983), mentioned in Sanskrit literature (Varma, 1970), corroborated by ethnographic studies (López-Prat et al., 2021), and seemingly indicated by the QT2 sample (Figure 6). This procedure could be related to a technical requirement mainly linked to the camouflage of craquelures in the finishing clay layers, as the ethnographical studies suggests (see Figure S5).

CONCLUSIONS

The analyses carried out on samples from the archaeological sites of Tepe Narenj and Qol-e-tut (Kabul, Afghanistan) have provided a better understanding of the technology production of their sculptural decoration. In this sense, the study of the information provided by Sanskrit literature and the Bengali contemporary tradition that deal with the making of terracruda sculptures have allowed us to outline some of the questions to be asked and in some cases provided keys to interpret the data.

Although the mineralogical and petrographic results seem to indicate a common extraction quarry, there are some relevant differences in the treatment of the clays depending on whether they belong to sculpture fragments, wall paintings, reliefs, or walls. The sculpture samples in particular show different overlapped layers of clay-based pastes with differences between the inner and outer layers, something stated in Sanskrit literature (Varma, 1970) and documented ethnographically (López-Prat et al., 2021). In parallel, epifluorescence and GC/MS analyses suggest that the different modeling and finishing layers of terracruda sculptures may contain an organic binder of potential plant origin. In the future, further studies that allow the study of all the samples with these techniques and a better understanding of the organic binders used should be performed. This is particularly interesting, because the use of adhesive substances of organic origin for the elaboration of modeling and finishing sculpture pastes is also mentioned in Sanskrit literature (Varma, 1970), and it is ethnographically observed in West Bengal, in the latter case exclusively when preparing the final stucco layer prior to polychromies (López-Prat et al., 2021).

The results obtained allow us to suggest that, in spite of the temporal and spatial amplitude and the different sources studied, there are common features in the making of the terracruda sculptures found in the Buddhist temples of Tepe Narenj and Qol-e-tut (fifth–11th c. CE), those described in the Sanskrit literature and the current Indian traditional knowledge. This issue deserves to be studied in depth as it would be a great advance toward a better knowledge of this type of sculpture characteristic of the Silk Roads.

ACKNOWLEDGEMENTS

This work is part of M. Lopez-Prat doctoral research and the Juan de la Cierva contract (FJC2021-046803-I) funded by MCIN (Ministerio de Ciencia e Innovación)/AE (Agencia Estatal de Investigación); 10.13039/501100011033) and by the European Union "Next Generation EU"/ PRT. The results have been obtained in the framework of the activities of the DIBEST department of the University of Calabria, the ERAAUB (a recognized and financed research group of the Generalitat de Catalunya - 2021 SGR 00696), the Institut d'Arqueologia of the Universitat de Barcelona, the Conservació-Restauració del Patrimoni research group (a recognized research group of the Generalitat de Catalunya-2021 SGR 00089), and the CASEs research group (a recognized and financed research group of the Generalitat de Catalunya–2021 SGR-00950). We gratefully acknowledge Zafar Paiman, who explained the details of his studies in Tepe-Narenj and Qol-e-tut, Susan Bean, for sharing her knowledge on Indian terracruda sculpture, and all the Bengali artists (specially the kumors of Kumortuli) who, in keeping with their ancient tradition, have collaborated to understand the manufacturing process of modeling terracruda sculptures. Many thanks to all the people and institutions involved in this transboundary east–west research, and specially to an explorer met in Samarkand.

PEER REVIEW

The peer review history for this article is available at https://www.webofscience.com/api/gateway/wos/peer-review/10.1111/arcm.12922.

DATA AVAILABILITY STATEMENT

The data that support the findings of this study are available 10.5281/zenodo.7634917.

ORCID

Monica López-Prat https://orcid.org/0000-0002-7026-5720

REFERENCES

Barthoux, J. (1930). Les Fouilles de Hadda III - Figures et Figurines. Album Photographique. Memoires de la Delegation Archeologique Française en Afghanistan. Paris et Bruxelles. Les Éditions G. Van Oest.

Bayerová, T., Gruber, M., & Krist, G. (2010). Technical study of polychrome clay sculptures from the Buddhist temple complex at Nako, Himachal Pradesh, North India». Multidisciplinary conservation: A holistic view for historic interiors (Rome, 23-24 march 2010) - joint interim meeting of five icom-cc working groups, *Sculpture, Polychromy, and Architectural Decoration*, 1-11.

Bernard, P. (1969). Quatrieme Campagne de Fouilles à Ai Khanoum (Bactriane). *Comptes Rendus des Séances de l'Académie des Inscriptions et Belles-Lettres*, *3*, 313–355.

Blänsdorf, C., & Melzl, E. (2009). *Technique of modelling the Buddha statues, the Giant Buddhas of Bamiyan: Safeguarding the remains, monuments and sites XIX* (pp. 201–214). ICOMOS.

Boggs, S. Jr. (2010). *Petrology of sedimentary rocks* (2nd ed.). Cambridge University Press.

Bonaduce, I., Cito, M., Colombini, M. P., & Lluveras, A. (2009). The characterisation of the organic binders. In M. Petzet (Ed.), *The Giant Buddhas of Bamiyan: Safeguarding the remains, Monuments and Sites XIX* (pp. 265–279). ICOMOS.

Chiari, G. (1993). Investigation and restoration of clay fragmentary statues from old Nisa, Turkmenistan. *7a Conferencia Internacional sobre O Estudio e Conservaçao Da Arquitectura de Terra, Silves* (Portugal): 228–230.

Correa-Ascencio, M., & Evershed, R. P. (2014). High throughput screening of organic residues in archaeological potsherds using direct acidified methanol extraction. *Analytical Methods*, *6*, 1330. https://doi.org/10.1039/c3ay41678j

Forgione, G. (2019). Clays and colours: Tracking technologies and theories of vision in the ancient Buddhist art of Afghanistan. *Restauro Archeologico*, *1*, 130–141.

Hammann, S., Cramp, L. J. E., Whittle, M., & Evershed, R. P. (2018). Cholesterol degradation in archaeological pottery mediated by fired clay and fatty acid pro-oxidants. *Tetrahedron Letters*, *59*, 4401–4404. https://doi.org/10.1016/j.tetlet.2018.10.071

Jerram, D. A. (2001). Visual comparators for degree of grain-size sorting in two and three-dimensions. *Computers & Geoscience*, *27*, 485–492. https://doi.org/10.1016/S0098-3004(00)00077-7

Klimburg-Salter, D. (2018). Contextualizing Mes Aynak. *Afghanistan*, *1*(2), 213–238. https://doi.org/10.3366/afg.2018.0015

Lluveras-Tenorio, A., Andreotti, A., Talarico, F., Legnaioli, S., Olivieri, L. M., Colombini, M. P., Bonaduce, I., & Pannuzi, S. (2022). An insight into Gandharan art: Materials and techniques of polychrome decoration. *Heritage*, *5*(1), 488–508. https://doi.org/10.3390/heritage5010028

López-Prat, M., Agostino, R. G., Bandyopadhyay, S. R., Carrascosa, B., Crocco, M. C., De Luca, R., Filosa, R., Formoso, V., Lancelotti, C., Noori, A. N., Pecci, A., Simón-Cortés, J., & Miriello, D. (2022). Architectural terracruda sculptures of the silk roads: New conservation insights through a diagnostic approach based on non-destructive X-ray micro-computed tomography. *Studies in Conservation*, *67*(4), 209–221. https://doi.org/10.1080/00393630.2020.1862605

López-Prat, M., Carrascosa, B., Miriello, D., Simón-Cortés, J., & Bandyopadhyay, S. R. (2021). An ethnographic approach to developing new conservation strategies for the archaeological clay-based sculpture of the Silk Road. In *Transcending Boundaries: Integrated Approaches to Conservation. ICOM-CC 19th Triennial Conference Preprints, Beijing, 17–21 May 2021*. Paris: International Council of Museums.

López-Prat, M., Lancelotti, C., Campo-Francés, G., Ray Bandyopadhyay, S., Carrascosa, B., Noori, N. A., Pecci, A., Simón-Cortés, J., & Miriello, D. (2022). The role of plants and fibres in modelling monumental terracruda sculptures of the silk roads: Archaeobotanical analyses from the Buddhists sites of Tepe-Narenj and Qol-e-tut (Kabul, Afghanistan). *Heritage Science*, *10*(1), 1–16. https://doi.org/10.1186/s40494-022-00709-2

Middleton, P., & Gill, A. (1996). Technical examination and conservation of the stucco sculture. *Catalogue of the Gandhara Sculpture in the British Museum*, *1*, 363–368.

Neuweiler, F., & Reitner, J. (1995). Epifluorescence microscopy of selected automicrites from lower Carnian Cipit boulders of the Cassian formation (Seeland Alpe, Dolomites). *Facies*, *32*, 26–28.

Paiman, Z. (2010). Kaboul: Les Bouddhas Colorés Des Monastères. *Archeologia*, *473*, 52–65.

Paiman, Z. (2012). Tepe Narenj: A Royal Monastery on the high ground of Kabul. *Journal of Inner Asian Art and Archaeology*, *5*, 33–58.

Paiman, Z. (2018). Le monastère de Qol-e-Tut à la lumière des fouilles archéologiques. *Afghanistan*, *1*, 95–121. https://doi.org/10.3366/afg.2018.0007

Pannuzi, S., Talarico, F., Guida, G., & Rosa, C. (2019). Polychromy and gilding in the Gandharan sculptures from Pakistan and Afghanistan: Samplings from Museum Guimet in Paris, Civic Archaeological Museum of Milan and Museum of Oriental Art of Turin. *Restauro Archeologico*, *1*, 40–81.

Pecci, A., Borgna, E., Mileto, S., Dalla Longa, E., Bosi, G., Florenzano, A., Mercuri, A. M., Corazza, S., Marchesini, M., & Vidale, M. (2020). Wine consumption in bronze age Italy: Combining organic residue analysis, botanical data and ceramic variability. *Journal of Archaeological Science*, *123*, 105256. https://doi.org/10.1016/j.jas.2020.105256

Pecci, A., Giorgi, G., Salvini, L., & Cau, M. A. (2013). Identifying wine markers in ceramics and plasters with gas chromatography - mass spectrometry. Experimental, ethnoarchaeological and archaeological materials. *Journal of Archaeological Science*, *40*, 109–115. https://doi.org/10.1016/j.jas.2012.05.001

Pias, J. (1976). *Formations superficielles et Sols d'Afghanistan* (pp. 17–50). Q.R.S.T.O.M. - C.N.R.S.

Powers, M. C. (1953). A new roundness scale for sedimentary particles. *Journal of Sedimentary Research*, *23*(2), 117–119.

Ricci, L. F. (1980). *Sedimentologia parte I: Materiali e tessiture dei sedimenti*. Bologna Clueb.

Russo, F., Neri, C., Mastandrea, A., & Baracca, A. (1997). The mud mound nature of the Cassian platform margins of the Dolomites, a case history: The Cipit boulders from Punta Grohmann (Sasso Piatto massif, northern Italy). *Facies*, *36*, 25–36. https://doi.org/10.1007/BF02536875

Tarzi, Z. (1986). La technique du modelage en argile en Asie Centrale et au Nord-Ouest de l'Inde sous les Kouchans: La continuité malgré les ruptures. *Ktéma*, *11*, 57–93. https://doi.org/10.3406/ktema.1986.2635

Varma, K. M. (1970). *The Indian technique of clay modelling*. Santiniketan.

Varma, K. M. (1987). *Technique of Gandharan and Indo-Afghan stucco images*. Proddu.

Verardi, G. (1983). Osservazioni sulla coroplastica di epoca kushana nel nord ovest e in Afghanistan in relazione al materiale di Tapa Sardar, seguite da una precisazione sulla natura e la data delle sculture di Ushkur. *Annali*, 43–3, Istituto Universitario.

Verri, G., Luczanits, C., Borges, V., Barnard, N., & Clarke, J. (2019). Investigations of a Gandharan stucco head of the Buddha at the Victoria and Albert Museum (IM.3-1931). *Technè*, *48*, 136–149.

Wentworth, C. K. (1922). A scale of grade and class terms for clastic sediments. *Journal of Journal of Geology*, *30*, 377–392. https://doi.org/10.1086/622910

Zhao, L. (2014). Selection of consolidants for the polychrome clay sculptures in the Guanyin Temple, Sichuan, China. *Studies in Conservation*, *59*(1), 289–291.

SUPPORTING INFORMATION

Additional supporting information can be found online in the Supporting Information section at the end of this article.

How to cite this article: López-Prat, M., De Luca, R., Pecci, A., Mileto, S., Bandyopadhyay, S. R., Bloise, A., Guido, A., Cipriani, M., Lancelotti, C., Carrascosa, B., Noori, N. A., Simón-Cortés, J.-M., & Miriello, D. (2024). The modeling pastes of the monumental *terracruda* sculpture of the Silk Roads: Archaeometric study of the Tepe Narenj and Qol-e-tut examples (Kabul, Afghanistan). *Archaeometry*, *66*(1), 76–99. https://doi.org/10.1111/arcm.12922